



Quarantine in a multi-species epidemic model with spatial dynamics

Julien Arino ^{a,*}, Richard Jordan ^b, P. van den Driessche ^c

^a *Department of Mathematics and Statistics, McMaster University, Hamilton, ON, Canada L8S 4K7*

^b *Department of Mathematics and Statistics, Mount Holyoke College, South Hadley, MA 01075, USA*

^c *Department of Mathematics and Statistics, University of Victoria, Victoria, BC, Canada V8W 3P4*

Received 31 March 2004; received in revised form 17 August 2005; accepted 15 September 2005

Available online 15 December 2005

Abstract

Motivation is provided for the development of infectious disease models that incorporate the movement of individuals over a range of spatial scales. A general model is formulated for a disease that can be transmitted between different species and multiple patches, and the behavior of the system is investigated in the case in which the spatial component consists of a ring of patches. The influence of various parameters on the spatial and temporal spread of the disease is studied numerically, with particular focus on the role of quarantine in the form of travel restriction.

© 2005 Elsevier Inc. All rights reserved.

1. Introduction

Epidemics have been observed and documented for millennia. While, traditionally, mathematical models of disease spread have tended to ignore or downplay spatial dynamics, the spatio-temporal

* Corresponding author. Present address: Department of Mathematics, University of Manitoba, 342 Machray Hall, Winnipeg, MB, Canada R3T 2N2. Tel.: +1 204 474 6927; fax: +1 204 474 7611.

E-mail addresses: arinoj@cc.umanitoba.ca (J. Arino), rjordan@mtholyoke.edu (R. Jordan), pvdd@math.uvic.ca (P. van den Driessche).

spread of epidemic diseases was noticed early on. Thucydides, himself a victim of the plague of Athens in 430 B.C. (and one of the few to later recover), reports [37] that

It first began, it is said, in the parts of Ethiopia above Egypt, and thence descended into Egypt and Libya and into most of the King's country. Suddenly falling upon Athens, it first attacked the population in Piraeus . . . and afterwards appeared in the upper city, when the deaths became much more frequent.

Since then, the spatial spread of infection has been observed many times. Notable examples include the Black Death (plague) in Europe in the 1300s, smallpox in the New World in the 1500s [26,47], followed by measles and diphtheria. More recently, HIV/AIDS which emerged in 1981, West Nile virus in North America in the late 1990s [31], and SARS in Asia in 2003 [45] have clearly exhibited spatial spread over vast regions, often jumping continents.

Some determining factors for spatial spread are well-understood, see, e.g. [3]. On a local scale, contacts between infective and susceptible individuals lead to the buildup of the epidemic. Then, on a somewhat larger scale, it is through contacts between individuals living in distinct, yet relatively close, regions that a disease becomes spatially mobile. However, with rapid, long distance travel of individuals (via airplane, for example), the situation is far more complicated.

Traditionally, models for the spatial spread of diseases employ partial differential equations. Typical assumptions are of two types; see [30] and the references therein. Either there is diffusion of infection-bearing individuals in a susceptible population, or the receptors of the disease are fixed and the infectious agent diffuses among them.

There are, however, important situations in which these approaches are not appropriate. One such situation concerns the spread of disease through sparsely populated regions. As an illustration, consider the Canadian province of British Columbia (BC), which has a surface area of 950 000 km², roughly the same as the combined surface area of France, Germany and the Netherlands (FGN). The population of BC is estimated, as of July 2004, at 4.2 million, whereas the combined population of FGN is 160 million. Moreover, there are 134 municipalities in BC versus 53 000 for FGN, and in BC more than 75% of the population lives in the areas of Greater Vancouver and Greater Victoria and in 9 other towns, each having more than 50 000 inhabitants. Compared to FGN, therefore, BC is a sparsely populated expanse of land with pockets of densely populated cities. While the diffusion approximation for spatial spread may be appropriate in individual, heavily populated cities in BC, it is clear that the rate of spread through less populated regions is quite different. At the very least, density-dependent (and either explicitly or implicitly spatially-dependent) diffusion coefficients are required to model the spread throughout the province. But even then, the model would not capture a situation where the disease jumps from one city to another before it spreads to regions in between.

Rapid transportation and, in particular, air travel, has changed the way epidemics spread. Whereas the well known case of the spread of rabies [30] is a perfect illustration of diffusion of infectious agents, the SARS epidemic in the spring of 2003 has made it clear that human diseases spread in a distinctly non-diffusive manner.

For diseases that involve several species that move at different rates and/or follow different migration patterns, it is all the more important to accurately model the spatial dynamics. Bubonic plague involving fleas, rodents and humans; and avian influenza involving poultry and humans are such examples. West Nile virus, the cycle of which involves birds and mosquitoes, is another

important example. The crucial role of species-dependent mobility rates and migration patterns can be highlighted by considering the foot-and-mouth disease outbreak in the UK in 2001 [14]. Cattle (and sheep) are very mobile, as they are frequently bought and sold. In the initial phase of the epidemic, before the disease was spotted, infected cattle were transported from farm to farm. After some infected cattle were diagnosed and the problem was recognized, it took some time until the political decision was made to ban all cattle movement in the UK. By that time, infected cattle had already been distributed between a large number of farms. The problem was exacerbated by the fact that humans, though not affected by the disease, could, and did, carry the virus from infected to uninfected herds. We can see, therefore, that in order to capture the spatial spread of foot-and-mouth disease, it is necessary to model the transportation networks along which cattle are transported between farms, and in addition, the model should include the unintentional spread of the disease by humans. The situation is similar for avian influenza. Infection can occur through contact of a bird with an infected bird, but also with infected manure; the latter can stay infected for months, and can be carried by wild birds or even humans [2]. For diseases that affect animals and insects (vectors) and can also be passed on to humans [44], it is important to accurately model not only the contact/mixing between humans and the various species, but also the movement patterns of each of the species involved, including that of humans.

Another source of heterogeneity in epidemics has its origin in social grouping. Mixing patterns can vary according to social groups, where this factor of aggregation should be considered in a very wide sense. Social patterns may differ from country to country or from region to region within a given country, leading to regional heterogeneities in contact or mixing structures (see, e.g. [36] for estimations of the mixing of populations with regards to AIDS in Western Europe). But the variations can occur on even finer scales; see, e.g. [41] for comparisons between five US cities, and [25] for observations on socio-economical determinants of the persistence of plague in a district of Tanzania. Other demographic and epidemiological parameters, such as lifespan, incubation and infectious periods can also be expected to vary geographically, as can the availability and type of intervention and control measures.

Geographic heterogeneities thus play a fundamental role in the spatial spread of infectious diseases. Nevertheless, much of classical mathematical epidemiology has tended to minimize geographic heterogeneity and related spatial aspects of deterministic epidemic models. One of the earliest exceptions is found in the work of Baroyan et al. [7,8] which considers the spatial spread of influenza between cities in the Soviet Union. In their approach, a large geographic region (country) is partitioned into smaller sub-regions (cities). Migration and transportation between these cities are explicitly incorporated, and within a given city disease transmission is modeled by a discrete deterministic compartmental SIR model. An SEIR (susceptible, exposed, infective and removed) version of this model was used recently [20] to study the spread of influenza between 52 major world cities. A model for the spread of influenza, using airline data for the 33 largest US cities for 1996–2001, has also been studied [24]. Grenfell et al. [21] used wavelet time series analysis to show that (in the pre-vaccine era) waves of measles infection moved regionally from large cities to smaller towns.

Recently, there has been increased interest in deterministic metapopulation disease models that do not reduce to the familiar reaction–diffusion systems. On the one hand, numerical integration of large systems of ordinary differential equations has now become efficient, owing to advances in computational power. This has led to a number of numerical investigations of spatial

metapopulation models. For example, Sattenspiel and Dietz [32] introduced a single species, multi-city epidemic model that describes the travel of individuals and keeps track of where an individual usually resides, as well as where an individual is at a given time. This model has subsequently been studied in various contexts; the effect of quarantine [33] and the influence of the mobility patterns [34] have been addressed. On the other hand, the introduction of the next generation operator [15] and the elucidation of its application to systems of ordinary differential equations [39], together with advances in the theory of persistence [46], have made it possible to obtain analytic results on this sort of model [4–6,17,18,42,43].

These deterministic, spatial disease models have the advantage that they allow for the investigation, either analytically or numerically, of various *spatio-temporal control* strategies. The oldest control method for the spatial spread of infectious diseases is *quarantine* through travel restrictions. A study of the impact on disease dynamics of this type of quarantine was undertaken by Sattenspiel and Herring [33], as applied to the model of [32]. Numerically this intervention method was shown to have little impact on the ultimate course of the epidemic.

We study the behavior of and the effect of quarantine in an SEIRS compartmental model for a multi-species disease with spatial dynamics; this is an extension of the SEIR model that we introduced previously [4]. Analytical results concerning the basic reproduction number \mathcal{R}_0 were obtained in [4], so we concentrate here on the transient behavior of the system with the spatial component consisting of a ring of patches. In Section 2, the model is described, and we briefly recall results from [4]. In Section 3, we study the numerical behavior of the system with the patches distributed in a ring. In Section 4, we consider the effect of quarantine in the model. Finally, in Section 5, we briefly consider the model in the context of avian influenza.

2. The model

To formulate a model involving s species occupying n spatial patches, let N_{ip} be the population number of species $i = 1, \dots, s$ in patch $p = 1, \dots, n$. For species i , the rate of travel or migration from patch q to patch p is denoted by $m_{ipq} \geq 0$. These rates form a non-negative matrix $\widehat{M}_i = [m_{ipq}]$ with $m_{ipp} = 0$. Assuming no birth or death during travel, the rate of change of N_{ip} , denoted by N'_{ip} , due to travel is given by

$$N'_{ip} = \sum_{q=1}^n m_{ipq} N_{iq} - \Gamma_{ip} N_{ip} \tag{2.1}$$

where $\Gamma_{ip} = \sum_{q=1}^n m_{iqp}$. Setting $N_i = [N_{i1}, \dots, N_{in}]^T$, where superscript T denotes transpose, gives the travel equation

$$N'_i = M_i N_i \tag{2.2}$$

with the mobility matrix $M_i = \widehat{M}_i - D_i$, where D_i is a diagonal matrix with Γ_{ip} as the (p,p) entry. From the sign pattern of M_i and the fact that each column sum is zero, it follows that $(-M_i)$ is a singular M-matrix; see, e.g. [16, Th. 5.11]. The non-zero entries of M_i specify the arcs of a directed graph for travel connections between the patches (as vertices). We assume here that there exists a path in the directed graph from patch p to patch q for all p, q , i.e., M_i is irreducible. More

generally, the patches can be divided into irreducible components for species i . From [4], it follows that the travel Eq. (2.2), with a non-negative initial condition and subject to the constraint of constant total population for species i , namely $\sum_{p=1}^n N_{ip} = N_i^0 > 0$, has a positive equilibrium $N_i^* = [N_{i1}^*, \dots, N_{in}^*]^T$ that is asymptotically stable.

In each of the n patches, a general SEIRS compartmental epidemic model for a disease that confers temporary immunity is formulated, with the numbers of susceptible, latent, infective (infectious) and recovered individuals of species i in patch p at time t denoted by S_{ip} , E_{ip} , I_{ip} and R_{ip} , respectively, thus $N_{ip} = S_{ip} + E_{ip} + I_{ip} + R_{ip}$. Newborns from species i in patch p enter the susceptible class with birth term $d_{ip}N_{ip}$, and the disease is transmitted horizontally within and between species according to standard incidence (see, e.g. [22,29]) with $\beta_{ijp} \geq 0$ the average number of adequate (disease transmitting) contacts per unit time in patch p between susceptibles of species i and infectives of species j . Rates of travel are assumed to be independent of disease status, and disease related death is neglected. Assuming exponential distributions for the time spent in each compartment, the average lifetime, latent period, infectious period and immune period for species i in patch p are denoted by $1/d_{ip}$, $1/\varepsilon_{ip}$, $1/\gamma_{ip}$ and $1/v_{ip}$, respectively, with these parameters positive. These assumptions lead to the following system of $4sn$ equations for species $i = 1, \dots, s$ in patch $p = 1, \dots, n$.

$$S'_{ip} = d_{ip}(N_{ip} - S_{ip}) + v_{ip}R_{ip} - \sum_{j=1}^s \beta_{ijp} S_{ip} \frac{I_{jp}}{N_{jp}} + \sum_{q=1}^n m_{ipq} S_{iq} - \Gamma_{ip} S_{ip} \quad (2.3a)$$

$$E'_{ip} = \sum_{j=1}^s \beta_{ijp} S_{ip} \frac{I_{jp}}{N_{jp}} - (d_{ip} + \varepsilon_{ip})E_{ip} + \sum_{q=1}^n m_{ipq} E_{iq} - \Gamma_{ip} E_{ip} \quad (2.3b)$$

$$I'_{ip} = \varepsilon_{ip} E_{ip} - (d_{ip} + \gamma_{ip})I_{ip} + \sum_{q=1}^n m_{ipq} I_{iq} - \Gamma_{ip} I_{ip} \quad (2.3c)$$

$$R'_{ip} = \gamma_{ip} I_{ip} - (d_{ip} + v_{ip})R_{ip} + \sum_{q=1}^n m_{ipq} R_{iq} - \Gamma_{ip} R_{ip} \quad (2.3d)$$

The initial value problem given by (2.3) and initial conditions $S_{ip}, E_{ip}, I_{ip}, R_{ip} \geq 0$ (with at least one of the E_{ip} or I_{ip} positive) and $N_i^0 > 0$ at time $t = 0$ is well posed, with all variables non-negative for $t \geq 0$.

A similar model, but for a disease with no recovery ($v_{ip} = 0$) was formulated in [4], and we briefly recall some results from [4] for M_i irreducible, that also apply to the model formulated above. If the system is at an equilibrium (i.e., all time derivatives are zero), and there is no disease in patch p , then there is no disease in any patch, that is the system is at the disease-free equilibrium (DFE). If the system is at an equilibrium and the disease is endemic in patch p (i.e., $E_{ip} + I_{ip} > 0$ for some i), then the disease is at an endemic equilibrium in all patches.

For system (2.3), the DFE always exists with $S_{ip} = N_{ip}^*$, $E_{ip} = I_{ip} = R_{ip} = 0$. To study its stability and hence determine whether the disease can invade the population, we proceed as follows. Let

$$F = \begin{bmatrix} 0 & G \\ 0 & 0 \end{bmatrix}$$

with $G = \bigoplus_{k=1}^n G_k$, where \bigoplus denotes direct sum,

$$V = \left[\begin{array}{c|c} A & 0 \\ \hline -C & B \end{array} \right]$$

with

$$A = \left[\begin{array}{c|c|c} A_{11} & \cdots & A_{1n} \\ \hline \vdots & \ddots & \vdots \\ \hline A_{n1} & \cdots & A_{nn} \end{array} \right], \quad B = \left[\begin{array}{c|c|c} B_{11} & \cdots & B_{1n} \\ \hline \vdots & \ddots & \vdots \\ \hline B_{n1} & \cdots & B_{nn} \end{array} \right], \quad \text{and } C = \bigoplus_{k=1}^n C_k$$

Here G_k, A_{jk}, B_{jk}, C_k are $s \times s$ matrices, with A_{jk}, B_{jk}, C_k diagonal. Matrix G_k has (i, j) entry equal to $\beta_{ijk} N_{ik}^* / N_{jk}^*$, the (i, i) entry of A_{kk} is equal to $d_{ik} + \varepsilon_{ik} + \sum_{l=1}^n m_{ilk}$, whereas for $j \neq k$ the (i, i) entry of A_{jk} is $-m_{ijk}$. Matrix B is the same as A but with ε_{ik} replaced by γ_{ik} . Finally, C_k has (i, i) entry equal to ε_{ik} . From their sign pattern, and the fact that they are diagonally dominant by columns, A and B are non-singular M-matrices [9, Ch. 6], thus A^{-1} and B^{-1} are non-negative. Using the results in [39], we obtain a formula for the basic reproduction number \mathcal{R}_0 , and the following stability result [4].

Theorem 2.1. For model (2.3) with s species and n patches,

$$\mathcal{R}_0 = \rho(GB^{-1}CA^{-1})$$

where ρ denotes the spectral radius. If $\mathcal{R}_0 < 1$, then the DFE is globally asymptotically stable, if $\mathcal{R}_0 > 1$ then the DFE is unstable.

Note that $GB^{-1}CA^{-1}$ is a non-negative matrix, which implies that its spectral radius is attained at the largest real eigenvalue. Here, the matrix G represents the disease transmitting contacts per unit time, B^{-1} gives the average sojourn time in the infective compartment, A^{-1} gives the average time of sojourn in the exposed compartment, whereas C represents the rate at which exposed individuals become infectives, thus CA^{-1} is a measure of the proportion surviving the exposed compartment. In general, \mathcal{R}_0 depends on the demographic, disease and mobility parameters. This dependence is quite complex, and is difficult to study analytically even in the case of one species on two patches; see [4] for some results in this direction.

3. Behavior of the epidemic in a ring of patches

We consider a restricted case of system (2.3) by supposing that the patches are arranged in a ring, and that migration can only take place between neighboring patches. We call *one-way* migration the case in which individuals in a given patch p can only migrate to patch $p + 1$, and from patch n to patch 1. In this case, for a given species i , $m_{i qp} > 0$ only if $p + 1 = q \text{ mod } n$, so that the matrix \widehat{M}_i only has the first subdiagonal and the $(1, n)$ entry non-zero. In the *two-way* migration case, individuals can also migrate from a given patch p to patch $p - 1$, and from patch 1 to patch n , giving a matrix \widehat{M}_i with first subdiagonal, first superdiagonal, $(1, n)$ and $(n, 1)$ entries non-zero.

The equilibrium value N_i^* of the population can be deduced explicitly, albeit messily, for this structure. Also, our model with this ring structure (with one- or two-way migration) closely mimics a one-dimensional partial differential equation (PDE) model with periodic boundary conditions. This allows us to compare the obtained behavior with that of a more classical reaction–diffusion PDE model.

We begin with the one species case (so drop the subscript i , and take $\beta_{ijp} = \beta_p$), and defer considerations on more than one species to Section 5, where an avian influenza-like situation is considered.

We choose a number n of patches sufficiently large so that the wave can fully develop before it reaches the last patch, but small enough so that simulations can be run very rapidly. In the simulations we use 15 patches ($n = 15$, hence 60 ODEs), but even on a personal computer, this number can easily be taken to be larger (integration for 500 days with $n = 500$ takes but a few minutes, for example). Initial populations are taken as 1000 individuals per patch and we assume that the infection starts in patch 1 with 100 infectives, i.e., $I_1(0) = 100$, $I_p(0) = 0$ for patches $p \neq 1$, and $S_p(0) = 1000 - I_p(0)$, $E_p(0) = R_p(0) = 0$ for all $p = 1, \dots, n$.

We choose the time unit to be a day, and except if otherwise noted, rate constants are expressed per day. In this section and the next, we take parameters compatible with influenza with $\beta_p = \beta$ for all $p \neq 1$, $\beta_1 > \beta$, and all other parameters equal in each patch, i.e., $d_p = d$, $v_p = v$, $\varepsilon_p = \varepsilon$, $\gamma_p = \gamma$. The average life expectancy $1/d$ is taken to be 75 years. The average incubation time $1/\varepsilon$ is 2 days, and the average infectious period $1/\gamma$ is 4 days. The immunity associated with influenza is a complex matter. It involves partial immunity to other influenza strains, and other mechanisms that are not well-understood. As we are considering the population regardless of which strain infects each individual, we make the simplifying assumption that the average immune period $1/v$ is one year, which is compatible with the observation that most individuals contract influenza at most once a year. Finally, we take $\beta = 0.5$ and $\beta_1 = 0.75$.

Fig. 1(a) and (b) are simulations of the model with the above parameters and one-way and two-way migration, respectively, with $m = m_{p+1,p} = 0.03$ and $m = m_{p,p+1} = m_{p+1,p} = 0.03$, respectively. In each case, there are several epidemic outbreaks (of diminishing intensity). For one-way migration (Fig. 1(a)), there is a second peak of infection that occurs after the first wave. This peak, which only takes place in patch 1 and several of its immediate successors, is a consequence of the ring structure chosen for these simulations. When the simulation starts, only patch 1 contains infectives. There is an initial steep drop in the number I_1 of infectives in this patch, as the susceptible population S_1 is not sufficient to sustain the epidemic. However, migration is simultaneously taking place, and individuals from every patch move to the next patch in the ring. Observation of patch 15 (the last patch) shows that the infective population is very low in this patch until about $t = 80$ days, when the epidemic wave finally reaches it. So until $t = 80$ days, most of the individuals migrating out of patch 15 are susceptibles. This inflow of susceptibles greatly slows down the decay of the epidemic in patch 1, and also replenishes S_1 enough that, when the epidemic wave completes its loop around the ring, there is a second major epidemic in patch 1. If the migration rate is large enough, then in some sense, patch 1 is overflowing with susceptibles, and some of them migrate into patch 2, etc. This leads to the second wave that can be observed in patches 2–4 in Fig. 1(a) around $t = 150$ days. On the other hand, if the migration rate is small ($m = 0.003$), then we observe less or even no propagation of this second major epidemic into the following patches, as can be seen after $t = 250$ in patch 1 in Fig. 2, but the first epidemic (the

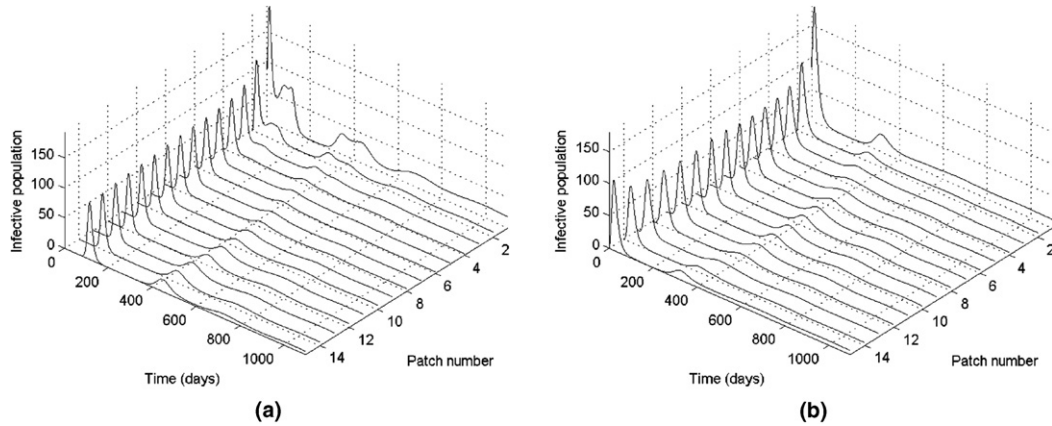


Fig. 1. Comparison of the behavior over three years of the epidemic on a ring of patches: (a) one-way migration; (b) two-way migration. Parameters are $n = 15$, migration $m = 0.03$, $\beta = 0.5$ (except $\beta_1 = 0.75$), $\varepsilon = 1/2$, $\gamma = 1/4$, $1/\nu = 1$ year and $1/d = 75$ years.

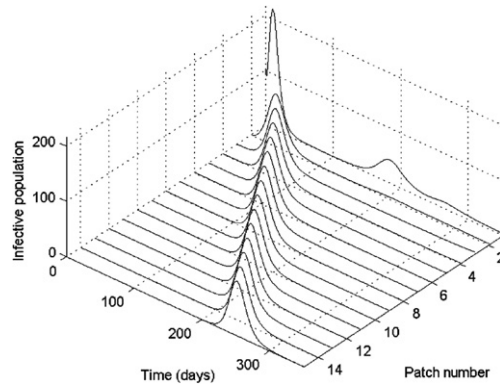


Fig. 2. Detail of the first epidemic wave for one-way migration. Small migration $m = 0.003$. Other parameters are as for Fig. 1.

one occurring in patch 1 at $t = 20$ days in Fig. 2) is more intense. For even smaller migration rates, e.g., $m = 0.0003$, the second major epidemic is barely noticeable or even absent.

Following this second epidemic wave, the numbers of individuals in the various epidemic states in the different patches have homogenized through diffusion (see Fig. 3(a)), and subsequent damped epidemic waves have a period about one year (i.e., comparable to $1/\nu$). The transient behavior we observe is compatible with results of PDE models (see, e.g. [1,23]).

In the case of two-way migration, as in Figs. 1(b) and 3(b), the diffusion of individuals through migration is faster. Fig. 3 shows details of the number of infectives per patch against time, for Fig. 1(a) and (b), when t varies between 200 and 1500 days. It is clear from these two figures that synchronization (through diffusion) is much faster in the two-way migration case.

Note that by choosing β_1 different from the other β , we avoid the situation described in [6, Corollary 7], where migration, be it one- or two-way, does not play a role in the value of \mathcal{R}_0 . Here, for

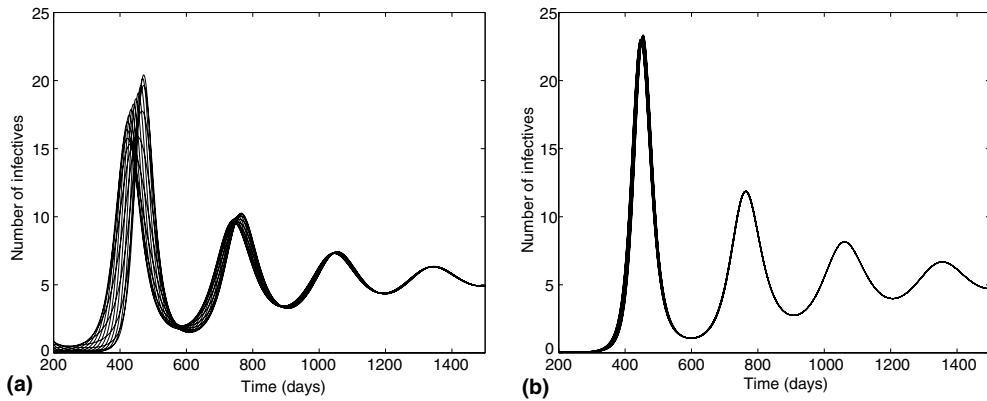


Fig. 3. Number of infectives per patch versus time for Fig. 1(a) and (b), showing synchronization between the patches, for t between 200 and 1500 days: (a) one-way migration; (b) two-way migration.

example, in the case of one-way migration, Fig. 1(a) has $\mathcal{R}_0 \simeq 2.53$, while Fig. 2 with its smaller migration rate has $\mathcal{R}_0 \simeq 2.95$.

Numerical results for an SEIR model (i.e., $v = 0$, corresponding to permanent immunity, which is appropriate for childhood diseases) are similar, except that there are no damped oscillations. The epidemic rises to a first peak and then goes monotonically to an equilibrium, which is either endemic or disease-free depending on the value of \mathcal{R}_0 .

4. Effect of quarantine

Quarantine can be of several types. We are solely concerned with travel or migration restrictions, which consist, as was the case during the SARS epidemic, in either advising or imposing a restriction of travel to certain destinations. In terms of cattle diseases, these correspond to movement restrictions, not to any culling that may take place simultaneously with movement restrictions. We are not concerned here with *isolation*, which consists in taking infectious or potentially infectious individuals out of the population to avoid further contaminations (see, e.g. [13] for SARS, [19] for HIV).

Quarantine is introduced in the model as follows. We assume that quarantining affects patches a to b , with $a \leq b$. For simplicity, we suppose that $1 < a \leq b < n$. We call patches 1 to $a - 1$ and $b + 1$ to n the non-quarantined section of the ring, and patches a to b the quarantined section of the ring. Migration from the non-quarantined section into the quarantined section, and from the quarantined section into the non-quarantined section, is reduced for species i by a factor $\bar{r}_i \in [0, 1]$. For $a < b$, within the quarantined section, migration is reduced by a factor $r_i^\circ \in [0, 1]$ for species i . Thus, $1 - \bar{r}_i$ and $1 - r_i^\circ$ are the external and internal quarantine efficacies, respectively. A quarantine efficacy of 0 has no effect on the migration, whereas a quarantine efficacy of 1 (perfect quarantine) results in the quarantined patches becoming geographically isolated from their neighbors.

Note that quarantine affects the value of N_i^* , but that the reasoning that led us to conclude the existence of a positive equilibrium for the travel equation in the general case is still valid here, so that the positive equilibrium N_i^* exists and is asymptotically stable. The quarantine reproduction

number \mathcal{R}_q can be calculated in the same way as \mathcal{R}_0 (Section 2, Theorem 2.1) by including the factors \bar{r} and \bar{r}^2 .

We start by studying the effect of quarantine on a single patch, i.e., $a = b$, in a ring with one-way migration, and for a single species. The following table shows the effect of preventive quarantine on a system of 15 patches. This type of quarantine could be termed *internally imposed quarantine*, and corresponds to a patch taking measures to protect itself from an incoming epidemic. In the simulations, we choose this patch to be $a = b = 7$. We use the following parameters. The migration rate between unquarantined patches is $m = 0.03$. The efficacy of the quarantine is indicated as the factor of this normal migration rate. The disease parameters are compatible with influenza data as given in Section 3. The simulation is run in all cases for $t_{\max} = 1000$ days. Let $I(t) = \sum_{i=1}^{15} I_i(t)$. The *average number of infectives* is given by the total number of cases divided by the time period, i.e., $\bar{I} = 1/t_{\max} \int_0^{t_{\max}} I(t) dt$. A numerical estimate of this value is obtained by computing the trapezoidal numerical integral of $I(t)$ over the interval of integration, using MatLab's `trapz` function. The $\min_i \bar{I}_i(t)$ and $\max_i \bar{I}_i(t)$ average numbers of infectives on any one patch are also given, where \bar{I}_i is the average number of infectives in patch i . The maximal instantaneous number of cases (infectives) is $\max_{t \in [0, 1000]} I(t)$.

Quarantine efficacy $1 - \bar{r}$	Average # inf. (min/max)	Max # of cases
0	112.8 (4/25)	193
0.5	112 (3.9/23.3)	193
0.9	108.9 (2.3/25.6)	221
0.999	106.2 (0.06/58.2)	250
1	98 (0/58.9)	251

We now proceed to the same kind of analysis, but with *externally imposed quarantine*. We use exactly the same parameters as in the previous type, but we suppose that the quarantine is applied instantaneously to the patch where the epidemic is initiated (patch 1). Since the contact parameter β_1 is different in patch 1, quarantining this patch results in variations of \mathcal{R}_q , which we show in the following table.

Quarantine efficacy $1 - \bar{r}$	Average # inf. (min/max)	Max # of cases	\mathcal{R}_q
0	112.8 (4.1/25)	193	2.53
0.5	113.9 (3.6/31.7)	207	2.75
0.9	116.8 (2.6/39.7)	363	2.95
0.999	106.7 (0.4/64.5)	515	3
1	9.9 (0/9.9)	220	N/A

When $1 - \bar{r} = 1$, then M is no longer irreducible, in the case of one-way migration. Thus, in the case of internally imposed quarantine, patch 7 is cut off from the patches that come before it, and so patches 7–15 have no infectives, while for externally imposed quarantine, patch 1 is cut off from the other patches, which do not have any infectives. Note also that in the case where the matrix is no longer irreducible, \mathcal{R}_q is only defined over the irreducible components, and thus there is no global value of \mathcal{R}_q .

In the case of imperfect quarantine, the main difference that is observed between the two types of quarantines is in the initial transients. If the system is run for a long time, then the average number of infectives obtained over the course of the simulation tends to the same value. The following table, where a quarantine efficacy of 0.999 is used, and all parameters are as previously stated, shows the average number of infectives in both types.

Final time (years)	Type of quarantine		Difference (%)
	Internally imposed	Externally imposed	
3	104.5846	100.3411	4.23
5	95.3228	94.0291	1.37
10	88.6263	87.893	0.83

For even larger (but unrealistic) final times, the difference between the two types of quarantines eventually goes to zero.

We now consider quarantine in a ring with two-way migration. In the following, $a = b = 7$, and the initial condition is taken in patch 1. The migration rates $m = m_{p,p+1} = m_{p+1,p} = 0.03$. All other parameters are taken exactly as in the one-way migration case. In the case of internally imposed quarantine, we have the following results.

Quarantine efficacy $1 - \bar{r}$	Average # inf. (Min/Max)	Max # of cases
0	114.4 (6.5/15.7)	180.5
0.5	114.3 (6.5/15.7)	180.5
0.9	114.3 (6.5/15.7)	180.5
0.999	114.1 (6.5/15.7)	180.5
1	107 (0/15.7)	180.5

Thus, in the case of two-way migration, imperfect travel restriction has virtually no effect. When travel restriction is perfect, the quarantined patch(es) have no disease. The situation is similar to one-way migration when $1 - \bar{r} = 1$, except that in the case of two-way migration, only patch 7 is cut off from the others and has zero infectives. Results for externally imposed quarantine for two-way migration are similar, and so are not reported here.

5. Avian influenza in a ring of patches

Avian influenza, also called fowl plague, is a disease of birds (see, e.g. [2,12]). It has two major forms. The first form, *low pathogenicity avian influenza* (LPAI), causes only a mild illness. The *highly pathogenic avian influenza* form is extremely contagious. It has a high mortality rate in many of the bird species it contaminates (although it seems to be more severe in the domestic populations than in the wild populations), with mortality rates reaching 100% in some cases [2]. Transmission of both forms to the human population has been observed [11,27,35,38].

We consider here a very simplified setting of LPAI in a ring of patches with one-way migration, with the system (2.3) taken in the case $s = 2$. For simplicity, we denote the species index as $1 = B$

for birds and $2 = H$ for humans. The mean duration of life is taken to be 75 years for humans, 2 years for a bird (which is compatible with most fowl species, for example). As with many diseases of livestock, the animal component of the disease has been the object of a lot of attention. The transmission from bird to bird has been estimated; in [40] the transmission coefficient was determined by experiments on chicken. A typical value of β was found to be 0.24 for LPAI; we use this value for β_{BBp} . This estimated value of 0.24 corresponds to a latent period of between one and two days. Therefore, we use the value $1/\varepsilon_B = 1.5$ days. From [40], the chicken that were infected by contact with inoculated chicken tested positive for LPAI during an average of 4.3 days (compared to 4.8 days for inoculated animals), so we use this value for $1/\gamma_B$. Parameters for humans are taken as in Sections 3, with $m_H = 0.03$. For birds, we take a migration rate $m_B = 0.1$. Note that in the case of birds, this is meant to account, for example, for movements due to sales.

The transmission probability from bird to human is less known. It has been hypothesized for example that in some cases, pigs can be intermediates between birds and humans [10]. On the other hand, in the case of infections in 1999 in Hong Kong, it was shown that transmission had been direct between birds and humans [28]. Since there are very few documented cases of transmission to humans, we suppose that $\beta_{HBp} = \beta_{BBp}/20$. Also, there are no documented cases of human to human transmission of LPAI, so $\beta_{HHp} = 0$. As mentioned in the Introduction, there are known cases where a human involuntary carried infected manure from one farm to another, spreading the infection. However, we do not model this possibility, and thus consider that humans cannot infect birds, $\beta_{BHp} = 0$.

Initial bird and human populations are taken as, respectively, 50 000 and 5000 per patch. Quarantine is applied to patch $a = b = 7$ with an efficacy of $1 - \bar{r}_B = 0.9$ for birds and $1 - \bar{r}_H = 0.5$ for humans. All other parameters are as previously used; we have a system of 120 ordinary differential equations. An example of the evolution of the number of infective individuals in the two species is shown in Fig. 4. In the case of the bird population of Fig. 4(a), the effect of the quarantine is invisible, as the two curves overlap. For the human population, the effect of the quarantine is to slow the epidemic, leading to lower infectious levels than in the case of no quarantine. However, the effect is reversed after a while, and for larger time, the two curves are indistinguishable.

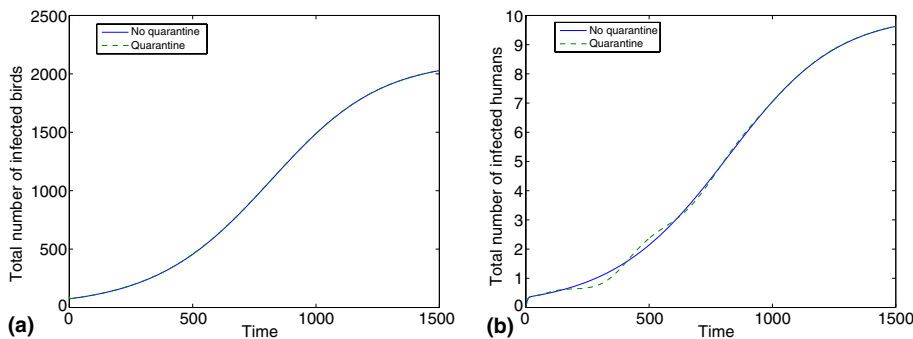


Fig. 4. Numbers of infective individuals in the two populations, with and without quarantine; one-way migration (a) bird population (b) human population. Quarantine of $\bar{r}_B = 0.1$ and $\bar{r}_H = 0.5$ in patch $a = b = 7$. All other parameters are as in the text. Note that the effect of quarantine on the bird population is not visible.

Clearly, even though there is no human to human transmission and the transmission probability from birds to humans is low, the disease is able to spread to all patches despite the restriction of travel. In the case of the parameters used here, we find $\mathcal{R}_0 = 1.024$, well in accordance with the values suggested in [40].

6. Discussion

We have investigated the impact of quarantine via travel restrictions in a multi-species, meta-population model of infectious disease spread. The aim has been to emphasize the importance of including geography in disease models and to illustrate one of many ways in which a model, such as the one developed in [4], may be used to probe the effectiveness of intervention and spatio-temporal control measures. As discussed in the Introduction, the development and analysis of such spatial models are still in their infancy stages. There are many possibilities for extending the model of Section 2 to increase realism. It is clear that for many human diseases of interest, the mobility/migration rates should be dependent upon whether an individual is infected (and symptomatic) or not. Someone who is in the infectious stage of SARS or influenza, for example, will typically be less mobile than an individual in the susceptible or latent stage of the diseases. From a modeling and simulation standpoint, it is easy to include these effects by allowing the migration rates to depend upon disease state, as in [42]. However, some methods and results presented in [4] and outlined here are not directly applicable.

It is worth noting, however, that for many animal diseases, such as bubonic plague and lyme disease, the mobility of the species involved is not expected to vary much according to disease state. Likewise, there are human-to-human transmitted diseases (such as the common cold) in which the symptoms exhibited by infectious individuals are sufficiently mild so as not to greatly impact their typical (meaning when they are healthy) mobility patterns (travel, commuting, etc). In such cases the rigorous theoretical results given here in Section 2 are applicable.

It is also important to investigate the impact of other intervention measures in the model, such as vaccination of susceptibles, rodent and/or vector control via culling (in the case of plague, for example), and alternate means of quarantine, such as isolation of infectious individuals and/or those who are known to have come in contact with an infectious individual. Because of the spatial component of our model, it is possible to explore the effects of applying control measures in restricted geographic regions or globally.

Spatial metapopulation models, such as the one we have presented here and those cited in the Introduction are ripe for extension and open up exciting new theoretical and numerical challenges. They allow the possibility of addressing a wide range of important and practical problems, only a few of which are described above.

Acknowledgment

J.A. dedicates this paper to Ovide. Research supported in part by NSERC and MITACS (P. van den Driessche).

References

- [1] G. Abramson, V.M. Kenkre, T.L. Yates, R.R. Parmenter, Travelling waves of infection in the hantavirus epidemics, *Bull. Math. Biol.* 65 (2003) 519.
- [2] D.J. Alexander, A review of avian influenza in different bird species, *Vet. Microbiol.* 74 (2000) 3.
- [3] J.J. Angulo, C.K. Takiguti, C.A.A. Pederneiras, P. Megale, Identification of pattern and process in the spread of a contagious disease, *Soc. Sci. Med.* 13D (1979) 183.
- [4] J. Arino, J.R. Davis, D. Hartley, R. Jordan, J.M. Miller, P. van den Driessche, A multi-species epidemic model with spatial dynamics, *Math. Med. Biol.* 22 (2) (2005) 129.
- [5] J. Arino, P. van den Driessche, The basic reproduction number in a multi-city compartmental epidemic model, *Lect. Notes Contr. Inf. Sci.* 294 (2003) 135.
- [6] J. Arino, P. van den Driessche, A multi-city epidemic model, *Math. Pop. Stud.* 10 (3) (2003) 175.
- [7] V.O. Baroyan, L.A. Rvachev, Deterministic epidemic models for a territory with a transport network, *Kibernetica* 3 (1967) 67.
- [8] V.O. Baroyan, L.A. Rvachev, U.V. Basilevsky, V.V. Ezmakov, K.D. Frank, M.A. Rvachev, V.A. Shaskov, Computer modeling of influenza epidemics for the whole country (USSR), *Adv. App. Prob.* 3 (1971) 224.
- [9] A. Berman, R.J. Plemmons, *Nonnegative Matrices in the Mathematical Sciences*, Academic Press, 1979.
- [10] I.H. Brown, The pig as an intermediate host for influenza A viruses between birds and humans, *Int. Congress Ser.* 1219 (2001) 173.
- [11] I. Capua, D.J. Alexander, Avian influenza and human health, *Acta Tropica* 83 (2002) 1.
- [12] I. Capua, D.J. Alexander, An update on avian influenza in poultry, *Int. Congress Ser.* 1263 (2004) 741.
- [13] G. Chowell, P.W. Fenimore, M.A. Castillo-Garsow, C. Castillo-Chavez, SARS outbreaks in Ontario, Hong Kong and Singapore: the role of diagnosis and isolation as a control mechanism, *J. Theor. Biol.* 224 (2003) 1.
- [14] G. Davies, The foot and mouth disease (FMD) epidemic in the United Kingdom 2001, *Comp. Immun. Microbiol. Infect. Dis.* 25 (2002) 331.
- [15] O. Diekmann, J.A.P. Heesterbeek, *Mathematical Epidemiology of Infectious Diseases: Model Building, Analysis and Interpretation*, Wiley, 2000.
- [16] M. Fiedler, *Special Matrices and their Applications in Numerical Mathematics*, Martinus Nijhoff Publishers, 1986.
- [17] E. Fromont, D. Pontier, M. Langlais, Disease propagation in connected host populations with density-dependent dynamics: the case of the Feline Leukemia Virus, *J. Theor. Biol.* 223 (2003) 465.
- [18] G.R. Fulford, M.G. Roberts, J.A.P. Heesterbeek, The metapopulation dynamics of an infectious disease: tuberculosis in possums, *Theor. Popul. Biol.* 61 (2002) 15.
- [19] J. Gani, S. Yakowitz, M. Blount, The spread and quarantine of HIV infection in a prison system, *SIAM J. Appl. Math.* 57 (6) (1997) 1510.
- [20] R.F. Grais, J.H. Ellis, G.E. Glass, Assessing the impact of airline travel on the geographic spread of pandemic influenza, *Eur. J. Epidemiol.* 18 (2003) 1065.
- [21] B.T. Grenfell, O.N. Bjørnstad, J. Kappey, Travelling waves and spatial hierarchies in measles epidemics, *Nature* 414 (2001) 716.
- [22] H.W. Hethcote, The mathematics of infectious diseases, *SIAM Rev.* 42 (4) (2000) 599.
- [23] F.M. Hilker, M. Langlais, S.V. Petrovskii, H. Malchow, A diffusive SI model with Allee effect and application to FIV, *Math. Biosci.* 206 (2007) 61.
- [24] J.M. Hyman, T. LaForce, Modeling the spread of influenza among cities, in: H. Banks, C. Castillo-Chavez (Eds.), *Bioterrorism*, SIAM, 2003, p. 215.
- [25] B.S. Kilonzo, Z.S.K. Mvena, R.S. Machangu, T.J. Mbise, Preliminary observations on factors responsible for long persistence and continued outbreaks of plague in Lushoto district, Tanzania, *Acta Tropica* 68 (1997) 215.
- [26] G.C. Kohn, *Encyclopedia of Plague and Pestilence*, Wordsworth, 1998.
- [27] M. Koopmans, B. Wilbrink, M. Conyn, G. Natrop, H. van der Nat, H. Vennema, A. Meijer, J. van Steenberghe, R. Fouchier, A. Osterhaus, A. Bosman, Transmission of H7N7 avian influenza A virus to human beings during a large outbreak in commercial poultry farms in the Netherlands, *The Lancet* 363 (2004) 587.
- [28] Y.P. Lin, W. Lim, V. Gregory, K. Cameron, M. Bennett, A. Hay, Recent examples of human infection by animal and avian influenza A viruses in Hong Kong, *Int. Congress Ser.* 1219 (2001) 179.

- [29] H. McCallum, N. Barlow, J. Hone, How should pathogen transmission be modelled, *Trends Ecol. Evol.* 16 (2001) 295.
- [30] J.D. Murray, *Mathematical Biology. II: Spatial Models and Biomedical Applications*, Springer, 2003.
- [31] L.R. Petersen, J.T. Roehrig, West Nile virus: a reemerging global pathogen, *Emerg. Inf. Dis.* 7 (2001) 611.
- [32] L. Sattenspiel, K. Dietz, A structured epidemic model incorporating geographic mobility among regions, *Math. Biosci.* 128 (1995) 71.
- [33] L. Sattenspiel, D.A. Herring, Simulating the effect of quarantine on the spread of the 1918–1919 flu in central Canada, *Bull. Math. Biol.* 65 (2003) 1.
- [34] L. Sattenspiel, A. Mobarry, D.A. Herring, Modeling the influence of settlement structure on the spread of influenza among communities, *Am. J. Human Biol.* 12 (2000) 736.
- [35] K. Subbarao, J. Katz, Avian influenza viruses infecting humans, *Cell. Mol. Life Sci.* 57 (2000) 1770.
- [36] R. Thomas, Estimated population mixing by country and risk cohort for the HIV/AIDS epidemic in Western Europe, *J. Geograph. Syst.* 3 (2001) 283.
- [37] Thucydides, *The History of the Peloponnesian War*. Circa 430 B.C. (The Internet Classics Archive Available from: <http://classics.mit.edu/Thucydides/pelopwar.html>).
- [38] M. Tollis, L. Di Trani, Recent developments in avian influenza research: epidemiology and immunoprophylaxis, *Vet. J.* 164 (2002) 202.
- [39] P. van den Driessche, J. Watmough, Reproduction numbers and sub-threshold endemic equilibria for compartmental models of disease transmission, *Math. Biosci.* 180 (2002) 29.
- [40] J.A. van der Goot, M.C.M. de Jong, G. Koch, M. van Boven, Comparison of the transmission characteristics of low and high pathogenicity avian influenza A virus (H5N2), *Epidemiol. Infect.* 131 (2003) 1003.
- [41] R. Wallace, D. Wallace, U.S. apartheid and the spread of AIDS to the suburbs: a multi-city analysis of the political economy of spatial epidemic threshold, *Soc. Sci. Med.* 41 (3) (1995) 333.
- [42] W. Wang, G. Mulone, Threshold of disease transmission in a patch environment, *J. Math. Anal. Appl.* 285 (2003) 321.
- [43] W. Wang, X.-Q. Zhao, An epidemic model in a patchy environment, *Math. Biosci.* 190 (1) (2004) 97.
- [44] R.A. Weiss, The Leeuwenhoek Lecture 2001. Animal origins of human infectious disease, *Phil. Trans. R. Soc. Lond. B* 356 (2001) 957.
- [45] World Health Organization, A multicentre collaboration to investigate the cause of severe acute respiratory syndrome, *Lancet* 361 (2003) 1730.
- [46] X. Zhao, *Dynamical Systems in Population Biology*, Springer, 2003.
- [47] H. Zinsser, *Rats, Lice and History: A Chronicle of Pestilence and Plagues*, Little Brown & Co., Boston, MA., 1935.